Dhaka Univ. J. Sci. 69(3): 179-185, 2022 (June)
Centennial Special Issue

ISSN 1022 - 2502, E-ISSN 2408-8528
DOI: https://doi.org/10.3329/dujs.v69i3.60028

# An Orbital Free Ab-initio Molecular Dynamics Study of Liquid Pt for Static and Dynamic Properties

**Mohammad Riazuddin Molla[1*, 2], G. M. Bhuiyan[1] and A .Z. Ziauddin Ahmed [1, 3]**

[1]*Department of Theoretical Physics, University of Dhaka, Dhaka-1000, Bangladesh*

[2]*Department of Mathematics, University of Dhaka, Dhaka-1000, Bangladesh*

[3]*Department of Basic Science, Primeasia University, Dhaka-1213, Bangladesh*

(Received : 18 November 2021 ; Accepted: 14 February 2022)

**Abstract**

Using the orbital free ab-initio molecular dynamics (OF-AIMD) simulation scheme we have examined the static and dynamic properties of liquid Pt at the thermodynamic state near to its melting point. In this simulation scheme, the Hohenberg and Kohn orbital free density functional theory (OF-DFT) has been employed. In OF-DFT, we have estimated the electron-ion interaction by a local pseudopotential and also controlled the exchange-correlation energy functional by using the local density approximation (LDA). The static properties, for instance, static structure factor, *S(q)*, pair correlation function, *g(r)*, coordination number, $N_c$, and isothermal compressibility, $\kappa_T$, are examined. Using the familiar single-particle dynamics, the self-diffusion coefficient and self-intermediate scattering function are studied. It is found that the self-intermediate scattering function is controlled by the self-diffusion coefficient. While for studying the collective dynamics of the system, we have calculated velocity of sound from the longitudinal dispersion relation and shear viscosity from the transverse current correlation function, $J_T(q, t)$. The OF-AIMD results are nicely fit with the theoretical and experimental results accessible to us for comparison.

**Keywords**: DFT, OF-AIMD, KS-AIMD, Static and Dynamic properties, Local Pseudopotential

## I. Introduction

To examine the properties of materials in the liquid state, the most consistent and very powerful method is the orbital free ab-initio molecular dynamics (OF-AIMD) technique. The Hohenberg and Kohn[1] version of orbital free density functional theory (OF-DFT) is applied to perform this simulation. The ground state electronic energy of a collection of atom for a given nuclear position is computed by OF-DFT where the forces on atoms are computed through the Hellmann-Feynman (HF) theorem. Consequently, it is possible to do MD simulation wherein the ionic position changes as classical systems but the electronic subsystem is monitored adiabatically. More detailed information can be found in the references[2-4]. The effective sp-electron valence, *Z,* has been considered to be a non-integral number which generally occurs due to sp-d hybridization effects[5-9]. Considering both technological and scientific outlook, platinum, **(**Pt**)** is an important transition metal[10]**.** In the electronics industry, Pt is utilized for making computer hard disks and thermocouples. It is also broadly used in jewelry. However, the main use of Pt is in catalytic converters for cars, trucks, and buses. The use of platinum compounds in chemotherapy drugs for cancer treatment is another important application of it[10]. Face-centered cubic(fcc) crystal structure Pt is found in the final column of group VIIIA of the periodic table having an atomic weight of 195.09 gm per mole. It has a material density of 21.45 gm/cm$^3$ and melting point 2041.40 K. The ionic number density of liquid Pt (*l*-Pt) at *T*=2053K is 0.0577Å$^{-3}$. Of late, González et al.[11] calculated some properties of *l*-Pt at $T = 2053$K by employing the Kohn and Sham ab-initio molecular dynamics (KS-AIMD) simulation technique using 120 particles. The atomic transport properties specifically diffusion coefficient and shear viscosity of *l*-Pt at temperature $T = 2053$K have been studied by Alemany et al.[12, 13] using classical molecular dynamics simulation. In this work Voter and Chen version of the embedded atom model (VC-EAM) potential, and a semiempirical many-body potential based on the second-moment approximation to the tight-binding method (TMM-SMA) are used. Availability of the KS-AIMD simulation results enables us to compare our OF-AIMD simulation data in this article. Both OF-AIMD and KS-AIMD are the first principle calculations but the first one is less expensive in terms of computational time than the second one. Interestingly OF-AIMD simulation method can handle hundreds or even thousands of particles whereas the KS-AIMD simulation method can handle only one or two hundred particles. For the first time, we have employed OF-AIMD simulation for the study of *l*-Pt taking 500 particles in the simulation box. The magnitudes obtained from the OF-AIMD calculation agreed well with the KS-AIMD results. No experimental data is available to us for the velocity of sound and self-diffusion coefficient at the thermodynamic state $T = 2053$K for comparison. Since there is no experimental data for the self-diffusion coefficient in the literature, we have computed it from the Stokes-Einstein relation[14] (see below) by using experimental values of shear viscosity[15] and experimental principal peak position[16], $r_p$ of $g(r)$. We observed a small

*Author for correspondence. e-mail: mriazmath@du.ac.bd

deviation between the diffusion coefficient that was calculated directly from the velocity autocorrelation function (VACF) and the empirical one that was calculated through the Stokes-Einstein relation by means of viscosity and principal peak position of *g(r)*. We have got two different values of experimental shear viscosity $\eta_{exp}$= 4.82 and 6.74 GPaps available in literature[15]. It is very much clear from our analysis that both OF-AIMD and KS-AIMD support former experimental data. On the other hand deviation of the latter one are almost 27% and 33% from KS-AIMD and OF-AIMD results respectively. There is not enough theoretical and experimental information available for the properties of *l*-Pt at *T*=2053K. We have got only one first principle calculation[11] available to compare with our study for the static and dynamic properties of *l*-Pt at *T*=2053K. For this reason, we have been interested to study some properties of *l*-Pt using a different approach which is computationally less expensive and reliable first principle calculation.

## II. Theories

*Density functional theory*

The total energy of a system can be defined as

$$E\left[n\left(\vec{r}\right)\right]=T_{\mathrm{s}}\left[n\right]+E_{\mathrm{H}}\left[n\right]+E_{\mathrm{xc}}\left[n\right]+E_{\mathrm{ext}}\left[n\right] \qquad (1)$$

by means of the density functional theory. In equation (1), $T_{\mathrm{s}}\left[n\right]$ represents the kinetic energy functional for non-interacting electrons, $E_{\mathrm{H}}\left[n\right]$ is the classical Hartree term, $E_{\mathrm{xc}}\left[n\right]$ is the exchange-correlation energy functional and $E_{\mathrm{ext}}\left[n\right]$ is the energy functional due to electron-ion interaction. Within the average density model[3, 17], the non-interacting kinetic energy functional, $T_{\mathrm{s}}\left[n\right]$, can be defined as

$T_{\mathrm{s}}\left[n\right]=T_{\mathrm{W}}\left[n\right]+T_{\alpha}\left[n\right]$,where;

$$T_{\mathrm{W}}\left[n\left(\vec{r}\right)\right]=\frac{1}{8}\int d\vec{r}\left|\nabla n\left(\vec{r}\right)\right|^{2}/n\left(\vec{r}\right) \qquad (2)$$

is the familiar von Weizsäcker term, and $T_{\alpha}\left[n\right]=\frac{3}{10}\int d\vec{r}\left[n\left(\vec{r}\right)\right]^{\frac{5}{3}-2\alpha}\left[\tilde{k}\left(\vec{r}\right)\right]^{2}$ with $\tilde{k}\left(\vec{r}\right)=\left(2k_{F}^{0}\right)^{3}\int d\vec{s}k(\vec{s})W_{\alpha}\left(2k_{F}^{0}\left|\vec{r}-\vec{s}\right|\right)$, $k\left(\vec{r}\right)=\left(3\pi^{2}\right)^{1/3}\left[n\left(\vec{r}\right)\right]^{\alpha}$. Additionally, $k_{F}^{0}$ represents the Fermi wave vector for an average electron density, $n_{e}=\frac{N_{e}}{V}$, and the weight function, $W_{\alpha}$ is considered for appropriate improvement of the linear response theory limit and Thomas-Fermi limit. More information can be obtained from reference[3, 17].

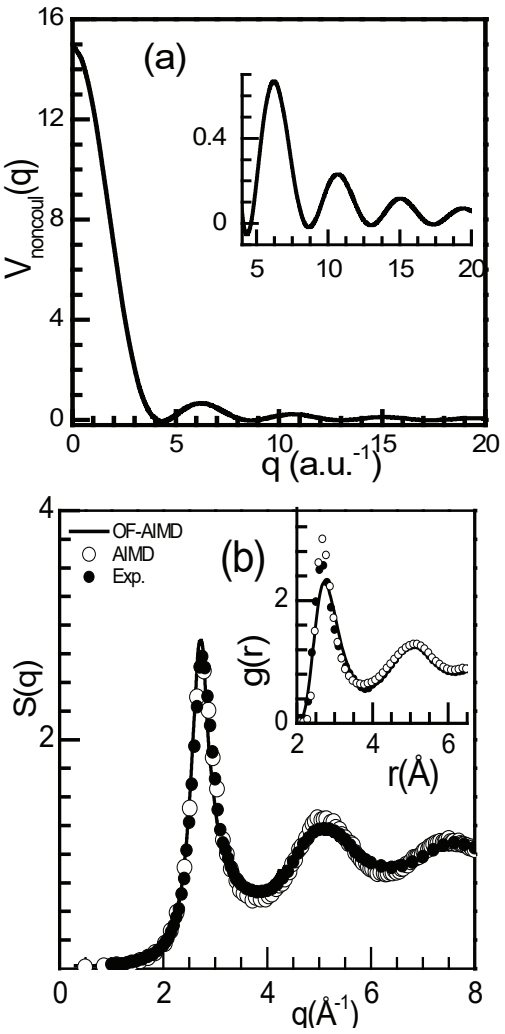


**Fig.1.** (a) The non- Coulombic part of the ionic pseudopotential for *l*-Pt at *T*=2053K. The inset displays a magnified phase of oscillations and (b)Static structure factor, *S(q)* with pair correlation function, *g(r)* (in the in set) at *T*=2053K for *l*-Pt.

*Pseudopotential*

Non-local pseudopotentials[18] are used for performing KS-DFT based AIMD simulations. To obtain the appropriate non-local pseudopotentials some properties are reproduced by fitting for a few others atom[17, 19, 20]. While the OF-DFT based AIMD namely OF-AIMD uses local pseudopotentials to approximate the electron-ion interaction. The form of the local ionic pseudopotential used in the present study has got the following form:

$$V_{ps}\left(r\right)=\begin{cases}H+Y\exp\left[-\dfrac{r}{g}\right] & \text{for} \quad r<R_{c}\\ -\dfrac{Z}{r} & \text{for} \quad r>R_{c}\end{cases} \qquad (3)$$

where *H* and *Y* are constants and $R_{c}$,*Z* and *g* denote the core radius, the effective number of nearly free sp-electrons, and

the softness parameter respectively. More details are given in reference[4, 17] of the local pseudopotential. Fig.1 (a) represents the non-Coulombic electron-ion interaction in $q$ space for *l*-Pt at *T*=2053K.

## III. Results and Discussions

The present OF-AIMD simulation has been performed for *l*-Pt at temperature, *T*=2053K having 500 particles in the periodic cubical cell. The cell size is calculated from the experimental ionic number density. The electronic energy functional is minimized with respect to $n(\vec{r}) = |\psi(\vec{r})|^2$ for the given ionic positions at time *t*, where $\psi(\vec{r})$ is the single effective orbital[3, 4]. The expansion of the orbital in plane waves is taken up to the value of cut-off energy, $E_{cut}$ = 20 Ryd. The quenching technique is applied for minimizing the energy of the system by means of the Fourier coefficients of $\psi(\vec{r})$ in every ionic step. The energy minimization gives the ground state valence electron density and energy. The forces on the ions from the electronic ground state energy are computed by using the Hellman-Feynman theorem. The ionic positions and velocities are updated from the solution of Newton's equations of motion through the Verlet leapfrog algorithm with finite time step $76\times10^{-4}$ ps. The OF-AIMD calculations were achieved by averaging over 5000 configurations for simulation time 38 ps. The static properties related to structure factor, pair correlation function, coordination number and isothermal compressibility are calculated. The value of $S(0)$ for calculating the isothermal compressibility is obtained from the long wave length limit of *S(q)*. The coordination number is calculated from *G(r),* which is known as the radial distribution function[16]. We have also calculated the single particle and collective dynamics for example diffusion coefficient, dynamic structure factor, velocity of sound and shear viscosity. The minimum iteration steps are found from good parameterizations of the pseudopotential. The pseudopotential parameters are chosen by considering the best overall fit to experimental data[16] for *S(q)* and we got the pseudopotential parameters namely core radius, $R_c$=1.45 au, softness parameter, *g*= 0.70 au, *sp*-electron occupancy number, *Z*=1.6. However, the Ewald radius is taken to be 5.00 au. The system required thermalization to compute the equilibrium properties. After the thermalization, the average values of temperature, energy and force continue to be constant over the range of 5000 configurations. This means that the system has been thermalized well and kept the system in its ground state during the whole simulation process.

*Static Properties*

The OF-AIMD static structure factor, *S(q)* for *l*-Pt at *T*=2053K and the XRD data of Waseda[16] are shown in Fig. 1(b). A fair agreement is found for both the positions and phase of the oscillations although a small deviation in height of the principal peak is observed. OF-AIMD *S(q)* principal peak height is approximately 4.5% higher than that of the experimental principal peak[15]. Fig. 1(b) reveals that *l*-Pt has a symmetric principal peak located at $q_p \approx 2.73$Å$^{-1}$ whereas the XRD principal peak position[16] of *S(q)* is located at $q_p \approx 2.76$Å$^{-1}$. If we compare the present OF-AIMD result *S(q)* with the AIMD calculations performed by González et al.[11], it appears clearly that the height and position of the principal peak and subsequent oscillations in the case of OF-AIMD *S(q)* is slightly better in agreement with the experiment. Here KS-AIMD[11] principal peak position is found at $q_p \approx 2.72$Å$^{-1}$ having underestimated height than OF-AIMD and experimental[16], *S(q)*. The value of *S(0)* is calculated by extrapolating the OF-AIMD *S(q)* for some small *q* values to $q \to 0$ using $S(q)=s_0+s_1q^2$. Then, the equation[21] $S(0)=\rho K_B T \kappa_T$, gives the isothermal compressibility, $\kappa_T$ =1.25±0.05(× $10^{-12}$ cm$^2$/dyne), where $K_B$ and *T* are Boltzman constant and temperature respectively. This value is reasonably closer to the experimental value $\kappa_T$ =1.44±0.32(×$10^{-12}$ cm$^2$/dyne), which is computed from the experimental[16], *S(q)* following the same procedure. While the KS-AIMD calculation performed by González et al.[11] yield a of value $\kappa_T$=1.80±0.15(×$10^{-12}$ cm$^2$/dyne).

The pair correlation function, *g(r)* is presented in the inset of Fig. 1(b) together with the XRD data[16] for *l*-Pt. Fig. 1 (b) shows a decent agreement with experiment[16], even if the height of the principal peak of OF-AIMD *g(r)* looks to be underestimated. It is worth noting that the principal peak positions of OF-AIMD and experimental[16] of *g(r)* are found at $r_p \approx 2.72$Å and $r_p \approx 2.70$Å, respectively. The principal peak position of *g(r)* calculated from KS-AIMD[11] is found at $r_p \approx 2.69$Å which is little underestimated from the experimental principal peak position[16]. The information of the coordination number is used for the structural study of non-crystalline materials. The coordination number, $N_c$ is calculated from the radial distribution function[16], $G(r)=4\pi\rho r^2 g(r)$,

$$N_c = \int_{r_0}^{r_m} 4\pi\rho r^2 g(r)\, dr \qquad (4)$$

where, $r_0 \approx 0$, $r_m \approx 3.74$Å and $\rho$ = 0.0577 Å$^{-3}$. The computed coordination number is $N_c \approx 12.34$, which is near to the experimental value[16], $N_c \approx 11.75$. González et al.[11] have computed, $N_c \approx 12.80$ from their study having $r_m \approx 3.77$Å of *g(r)*.

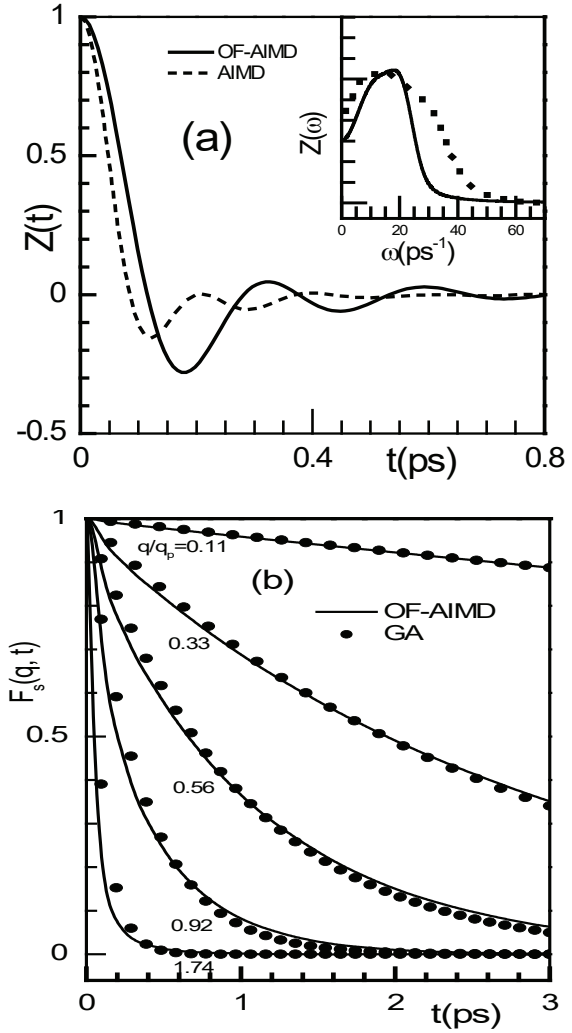


**Fig. 2.** (a) Normalized VACF, *Z(t)* of *l*-Pt with the power spectrum, $Z(\omega)$ (in the inset) of *Z(t)* (b) $F_s$ *(q, t)* for various values, $q/q_p$ of *l*-Pt at *T*=2053K with Gaussian approximation (GA) of $F_s$ *(q, t)*.

*Dynamic Properties*

Single Particle Dynamics

The normalized velocity autocorrelation function (VACF) defined by[21], $Z(t) = <\vec{v}(t).\vec{v}(0)> / <v^2>$ and the mean square displacement defined by $\langle \delta r^2(t) \rangle = \langle |\vec{r}(t) - \vec{r}(0)|^2 \rangle$ are used to calculate the self-diffusion coefficient in the present simulation. Using the Green-Kubo formula[21],

$$D = \frac{TK_B}{M} \int_0^\infty Z(t)\, dt \qquad (5)$$

and the famous Einstein relation[21],

$$D = \lim_{t\to\infty} \frac{\langle \delta r^2(t) \rangle}{6t}, \qquad (6)$$

we have computed the self-diffusion coefficient, $D$. In equation (5), $M$ is the mass of an atom. Both processes provide almost the same result. The plot of *Z(t)* for *l*-Pt at *T*=2053K calculated from the OF-AIMD and KS-AIMD[11] are shown in Fig. 2(a), where the usual cage effect is detected with a first minimum and the following oscillations of *Z(t)* seem to be weak for KS-AIMD[11] than it is detected in OF-AIMD. The negative values of *Z(t)* happen as a result of the backscattering effect which is made by the cage effect. The first minimum occurs in a shorter time for KS-AIMD than OF-AIMD and the depth is also lower for KS-AIMD[11]. For further details see references[3, 4]. Applying the processes stated above, the self-diffusion coefficient has been evaluated and we found $D$=0.33±0.01Å$^2$ps$^{-1}$. While the CMD study performed by Alemany et al.[12, 13] reported values $D$=0.281±0.003Å$^2$ps$^{-1}$ and $D$=0.284±0.003Å$^2$ps$^{-1}$. The KS-AIMD study of González et al.[11] reported a value $D$=0.27±0.02Å$^2$ps$^{-1}$. It seems that our OF-AIMD result for $D$ is comparable to the other calculated values[11-13]. There is no experimental value for the self-diffusion coefficient of *l*-Pt but there are two experimental[15] results for shear viscosity, $\eta_{exp}$ which are 4.82 and 6.74 GPaps. The experimental self-diffusion coefficient is evaluated from the Stokes-Einstein relation using the experimental values of shear viscosity and the principal peak position of experimental *g(r)*. Using the values of experimental shear viscosity, $\eta_{exp}$ = 4.82, 6.74 GPaps and the principal peak position of *g(r), d*=$r_p$=2.70Å we obtained $D$ = 0.35 Å$^2$ps$^{-1}$ and 0.25 Å$^2$ps$^{-1}$ from the Stokes-Einstein relation[14], respectively. Our OF-AIMD result for $D$ is nicely agreed with the first one, $\eta_{exp}$= 4.82 GPaps. On the other hand, the agreement of KS-AIMD[11] result for $D$ matches well with the second one, $\eta_{exp}$= 6.74 GPaps which is 27% larger than the shear viscosity obtained from KS-AIMD[11]. From Stokes-Einstein empirical relation[14] we have calculated diffusion coefficient, $D$=0.36 Å$^2$ps$^{-1}$ and 0.34 Å$^2$ps$^{-1}$ by using $\eta$ and $r_p$ obtained from OF-AIMD and KS-AIMD respectively. The empirical value of $D$=0.36 Å$^2$ps$^{-1}$ is reasonably good in agreement with the OF-AIMD value, $D$=0.33 Å$^2$ps$^{-1}$. We have also observed that the value of $D$=0.25Å$^2$ps$^{-1}$ calculated directly from KS-AIMD[11] VACF is almost 26% smaller than empirically found value $D$=0.34Å$^2$ps$^{-1}$.

In the present simulations, the self-intermediate scattering function, $F_s$ (*q, t*), is described as[3, 4] ,

$$F_s(q,t) = \frac{1}{N} < \sum_{j=1}^{N} \exp[i\vec{q}.\vec{R}_j(t+t_0)] \exp[-i\vec{q}.\vec{R}_j(t_0)] >, \qquad (7)$$

from which we get the proper knowledge of the single particle motion. This function also decides that the single particle dynamics are not identical in length scales, ranging from $q\to 0$ to $q\to\infty$, which are known to be the hydrodynamic limit and independent particle limit, respectively. The $F_s$ (*q, t*), is also defined by

$$F_s(q,t) = e^{-Dq^2 t}, \quad (8)$$

which is familiar as the Gaussian approximation (GA), where $D$ is recognized as the self-diffusion coefficient[21]. The self-intermediate scattering function, $F_s(q, t)$ of *l*-Pt, for various $q/q_p$ values are shown in Fig. 2(b). Where the continuous lines represent the OF-AIMD $F_s(q, t)$ as defined in equation (7) and the filled circles represent the Gaussian approximation for $F_s(q, t)$ as given by equation (8). Fig. 2(b) shows the usual monotonic non-linear decrease with time which falls faster with increasing $q/q_p$ values. Indeed, this movement is parallel to that of the simple liquid metals in the vicinity of their respective triple points[3, 4, 21, 22]. From the same Fig. 2(b), it also appears that equations (7) and (8) perfectly amalgamate with each other for low $q/q_p$ values which suggests that the $F_s(q, t)$ is organized by *D*. However, it deviates slightly at small *t* for larger values of $q/q_p$. This is obviously exposing the limitations of the Gaussian approximation.

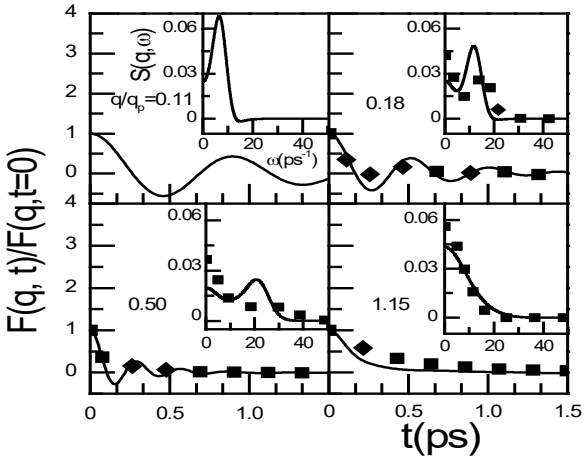


**Fig. 3.** Normalized *F(q,t)* for various values, $q/q_p$ of *l*-Pt at $T = 2053\text{K}$. The inset displays the corresponding dynamic structure factor, $S(q,\omega)$. Continuous line: OF- AIMD and Short dash line: KS-AIMD[11].

*Collective Dynamics*

The intermediate scattering function, $F(q,t)$ is described as[3, 4, 21]

$$F(q,t) = \left(\frac{1}{N}\right) < \sum_{j=1}^{N} \exp[i\vec{q}.\vec{R}_j(t+t_0)] \sum_{l=1}^{N} \exp[-i\vec{q}.\vec{R}_l(t_0)] >, \quad (9)$$

where, $N$ and $\vec{R}_j(t)$ are the whole number of particles and position of the *j*th ion at time *t*, respectively. It is a density-density correlation function from which one can get knowledge regarding the collective dynamics of density fluctuations over both the length and time scales. Results of *F(q,t)* from the present OF-AIMD simulation are illustrated in Fig. 3 along with KS-AIMD[11] $F(q,t)$. Our calculated, *F(q, t)* from OF-AIMD displays oscillatory behavior which persists up to $q \approx 0.73 q_p$ approximately and the amplitude of the oscillations being stronger for the smaller $q/q_p$ values. This is a usual behavior of simple liquid metals near melting as found in both simulations and theoretical models[3, 4, 21, 22]. Around $q/q_p \approx 1$, *F(q,t)* decline slowly which is known as "de Gennes narrowing". The dynamic structure factor $S(q,\omega)$ is directly connected with *F(q,t)*. The time Fourier transform of the *F(q,t)* with an appropriate window to smooth out truncation effects[21, 22] provides the dynamic structure factor, $S(q,\omega)$. The corresponding results of $S(q,\omega)$ are shown in the inset of Fig. 3 along with KS-AIMD results[11]. Where the dynamic structure factors, $S(q,\omega)$ obtained from both OF-AIMD and KS-AIMD[11] demonstrate well-defined side peaks for a small range of $q/q_p$ values due to collective density excitations. In particular, it is seen up to $q \approx 0.73 q_p$ in the case of OF-AIMD. Dynamic structure factor has an apparent tail with a clear starting point. In the free particle limit ($q \to \infty$), there are high-frequency peaks of $S(q, \omega)$ and these peaks do not occur in high-$\omega$ regions. Following distinct behavior of *F(q,t)* obtained from OF-AIMD and KS-AIMD are :

(i) The OF-AIMD *F(q,t)* oscillations have a larger period and higher amplitude.

(ii) The oscillatory activities of OF-AIMD *F(q,t)* are more clearly marked and the oscillations have vanished for larger $q / q_p$ values than KS-AIMD.

(iii) The OF-AIMD *F(q,t)* shows no weak diffusive performance like KS-AIMD.

(iv) However, the calculated OF-AIMD *F(q,t)* almost come to an agreement with the corresponding *F(q,t)* of KS-AIMD for $q / q_p \geq 1$.

The above variations are also visible in the corresponding dynamic structure factors, $S(q,\omega)$ which are represented for some $q/q_p$ values in the inset of Fig.3. Our calculated OF-AIMD $S(q,\omega)$ exhibits a clear side peak up to $q / q_p \approx 0.73$ and similar structures are also detected in the corresponding KS-AIMD $S(q,\omega)$ whereas their side peaks vanish at lower $q/q_p$ values. More excitingly, the position of the side peaks in OF-AIMD $S(q,\omega)$ is always found at a smaller $\omega$ value for any $q/q_p$ value.

The variable $\vec{J}(q,t) = \sum_{j=1}^{N} \vec{v}_j(t) e^{i\vec{q}.R_j(t)}$ is recognized as the current density linked with the overall motion of the particles. The variable $\vec{J}(q,t)$ can be divided as $,\vec{J}(q,t) = \vec{J}_L(q,t) + \vec{J}_T(q,t)$. Here $\vec{J}_L(q,t)$ and $\vec{J}_T(q,t)$ are the longitudinal component parallel to $\vec{q}$ and transverse component perpendicular to $\vec{q}$, respectively. The

longitudinal, $J_L(q,t)$, and transverse, $J_T(q,t)$, current correlation functions are defined as[3,21], $J_L(q,t)=\frac{1}{N}\left\langle \vec{J}_L^{*}(q,0).\vec{J}_L(q,t)\right\rangle$ and $J_T(q,t)=\frac{1}{2N}\left\langle \vec{J}_T^{*}(q,0).\vec{J}_T(q,t)\right\rangle$ respectively. The time Fourier transform of $J_L(q,t)$ and $J_T(q,t)$ gives spectra which are denoted by $J_L(q,\omega)$ and $J_T(q,\omega)$ respectively. The OF-AIMD $J_L(q,\omega)$ show a peak for all $q$ values and from the position of the side peak of $J_L(q,\omega)$, a dispersion relation for the longitudinal modes, $\omega_L(q)$ has been found and is presented in Fig. 4(a) along with KS-AIMD[11] results. The $q$ dependent adiabatic sound velocity, $c_s(q)$ is the slope of the curve, $\omega_L(q)$ at low $q$ region but in the limit $q\to 0$, the slope of the curve $\omega_L(q)$ yields the adiabatic sound velocity, $c_s$. We have taken the slope of the curve, $\omega_L(q)$ in the limit $q\to 0$ taking $q \le 0.84$ Å$^{-1}$ values of $\omega_L(q)$, then we get $c_s$=(2400±50)m/s. Whereas the experimental adiabatic sound velocity is $c_s$=3053m/s at the melting temperature[23].

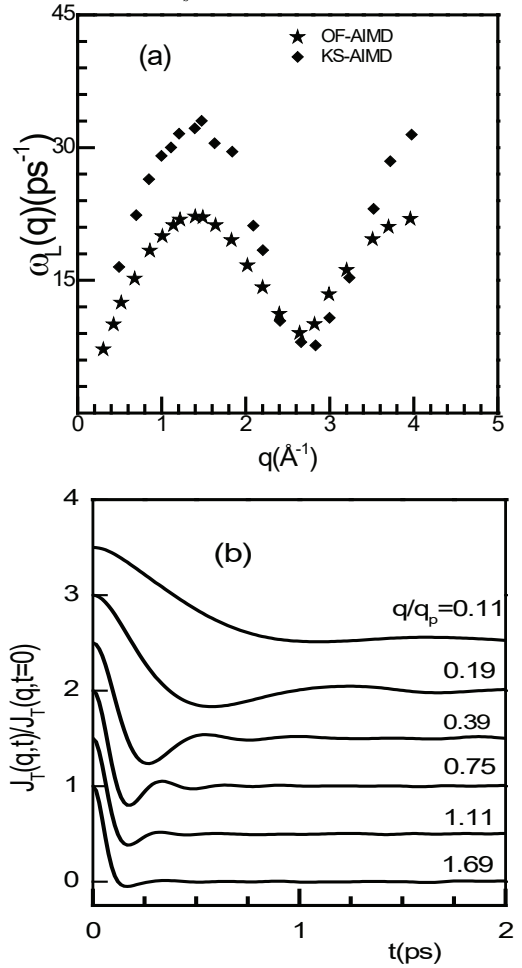


**Fig. 4.** (a) Longitudinal dispersion relation for *l*-Pt at $T$=2053K and (b) Normalized $J_T(q,t)$ at various values, $q/q_p$ of *l*-Pt at $T$=2053K.

We may note here that the KS-AIMD method[11] produces larger value of adiabatic sound velocity, $c_s$=(3000±150)m/s as compared to our result and close to experimental value measured at melting. On the other hand the Gitis-Mikhailov model and modified Einstein-Lindemann model[23] gave $c_s$=2193m/s and $c_s$=2713m/s, respectively, at the melting point. M. R. Molla[24] computed a reduced value $c_s$=(2184±24) m/s from the dispersion relation which is formed by the side peaks of the dynamic structure factors, $S(q,\omega)$. The value $q=0.305$Å$^{-1}$ is the least $q$ value obtained from the simulation. The OF-AIMD[24], $J_T(q,\omega)$ show a peak for some $q$ values starting from $q$=0.43Å$^{-1}$.

The shear viscosity, $\eta$ is computed from the transverse current correlation function, $J_T(q,t)$ because it carries information about the shear modes. The $J_T(q,t)$ is characterized as[3, 21]

$$J_T(q,t)=\frac{1}{N}\left\langle J^{*}_{x}(\vec{q},0)J_x(\vec{q},t)\right\rangle \qquad (10)$$

Eqn. (10) is not related to any computable quantity and it can only be gained from molecular dynamics simulations. The shear viscosity coefficient, $\eta$ is computed from the $J_T(q,t)$ by following the method described in[21,25,26]. The Laplace transform of $J_T(q, t)$ is denoted by $\tilde{J}_T(q,z)$ which is the memory function demonstration of $J_T(q,t)$ and it is defined as[21, 22],

$$\tilde{J}_T(q,z)=\frac{1}{\beta m}\left[z+\frac{q^2}{m\rho}\tilde{\eta}(q,z)\right]^{-1} \qquad (11)$$

where, $\tilde{\eta}(q,z)$ represents the generalized shear viscosity coefficient. We get $\beta m\tilde{J}_T(q,z=0)$ by taking the area covered by the normalized $J_T(q,t)$. Using the value $\beta m\tilde{J}_T(q,z=0)$ for each $q$ value, we get $\tilde{\eta}(q,z=0)$ from equation (11). Then the usual shear viscosity coefficient $\eta$ is obtained by extrapolating the values of $\tilde{\eta}(q,z=0)$ to $q$=0 and the calculated value of $\eta$ from OF-AIMD method is 4.60±0.49 GPaps. This value is very near to the value of $\eta$=4.90±0.25 GPaps, computed from KS-AIMD[11]. The experimental values[15] for liquid Pt are 4.82 and 6.74 GPaps. The first one is very near to our calculated value but the second one is nearer to the CMD simulation result[13], $\eta_{CMD}$=6.09±0.96 GPaps. The CMD simulation[12] along with EAM potential reported $\eta_{CMD}$=5.92±0.48 GPaps.

## IV. Conclusion

The orbital free ab-initio molecular dynamics simulation technique has been used to compute the static and dynamic

properties of *l*-Pt near the temperature of its melting point. The simulated static structure factor and pair correlation function, calculated by using the OF-AIMD, are better in agreement with the experimental data[16] and also with the results of KS-AIMD simulation[11] results. The evaluated values for the self-diffusion coefficient and shear viscosity are also found to be good in agreement when compared with the corresponding experimental data, and also with available CMD and KS-AIMD results[11-13]. The existence of clear side peaks in the calculated dynamic structure factors, $S(q,\omega)$, demonstrates the effect of collective excitation. The present orbital free scheme of simulation permits us to predict the static and dynamic structure factor of *l*-Pt with certain precision although it is started with a plane wave basis.

**Acknowledgment**

The authors express their deep gratitude to Professor Dr. D. J. González and Dr. L. E. González, Department of Theoretical Physics, University of Valladolid, Valladolid, Spain for providing orbital free ab-initio molecular dynamics (OF-AIMD) code to us.

**References**

1. Hohenberg P. and W. Kohn, 1964. Inhomogeneous Electron Gas.*Phys. Rev*., **136**, B864-B871.
2. Kohn W. and L. Sham, 1965. Self-Consistent Equations Including Exchange and Correlation Effects.*J. Phys. Rev.*, **140,** 1133- A1138.
3. González D. J., L. E. González, J. M. López andM. J. Stott, 2001.Orbital free *ab initio* molecular dynamics study of liquid Al near melting.*J. Chem. Phys.,***115**, 2373-2376.
4. Bhuiyan G. M., L. E. González and D. J. González, 2012. Orbital free ab initio molecular dynamics simulation study of some static and dynamic properties of liquid nobel metals. *Condensed Matter Phys.*, **15:3**, 33604:1-19.
5. Moriarty J. A., 1982.Density-functional formulation of the generalized pseudopotential theory. II.*Phys. Rev. B*,**26**, 1754-1780.
6. Moriarty J. A., 1988. Density-functional formulation of the generalized pseudopotential theory. III Transition-metal interatomic potentials.*Phys. Rev. B*,**28**, 3199-3231.
7. Moriarty J. A, 1990. Analytic representation of multi-ion interatomic potentials in transition metals.*Phys. Rev. B*,**42**, 1609-1628.
8. Gelatt C. D., Jr. H. Ehrenreich andR. E. Watson, 1977. Renormalized atoms: Cohesion in transition metals.*Phys. Rev. B*,**15**, 1613-1628.
9. Phuong L. Do., A. Pasturel and D. N. Manh, 1993.Effect of s-d hybridization on interatomic pair potentials of the 3d liquid transition metals.*J. Phys.: Condensed Matter*,**5**, 1901-1918.
10. Pocajt V., 2010. The world's most comprehensive materials database. *Total Materia*, **February**,1.
11. González L. E., D. J.González,M. R.Molla,A. Z. Z. Ahmed and G. M. Bhuiyan , 2017.Ab-initio study of several static and dynamic properties of liquid palladium and platinum.*EPJ Web of Conferences*, **151**, 03002:1-7.
12. Alemany M. M. G., C.Rey and L. J Galleogo, 1988. Transport coefficients of liquid transition metals: A computer simulation study using the embedded atom model. *J. Chem. Phys.*,**109,** 5175-5176.
13. Alemany M. M. G., O. Diéguez, C. Rey and L. J. Galleogo, 1999.Molecular-dynamics study of the dynamic properties of fcc transition and simple metals in the liquid phase using the second-moment approximation to the tight-binding method. *Phys. Rev. B*,**60**, 9208-9211.
14. Landau L. D, 1987. Fluid Mechanics, Pergamon, New York.
15. Iida T. and R. I. L., 1993. The Thermophysical Properties of Metallic Liquids, Oxford University Press, Oxford.
16. Waseda Y., 1980. The Structure of Non-crystalline Materials, McGraw-Hill Pub. Co., New York.
17. Bhuiyan G. M, L. E. González and D. J. González, 2011. An Orbital-free Molecular Dynamics Study of Static and Dynamic Properties of Liquid Sn. *Euro. Phys. J. Web of Conferences*, **15**, 01011:1-4.
18. Trouiller N. and J. L. Martins, 1991. Efficient pseudopotentials for plane-wave calculations. *Phys. Rev. B*, **43**, 1993-2006.
19. Caldeín L., L. E. Gonzálezand D. J. González, 2009. First-principles study of the layering at the free liquid Sn surface. *Phys. Rev. B*, **80**, 115403:1-7.
20. Itami T. S. Munejiri , T. Masaki , H. Aoki, Y. Ishil , T. Kamiyama, Y. Senda, F. Shimojo and K. Hoshino , 2003. Structure of liquid Sn over a wide temperature range from neutron scattering experiments and first-principles molecular dynamics simulation: A comprison to liquid Pb.*Phys. Rev. B*, **67,**064201:1-12.
21. Balucani U. and M. Zoppi, 1994. Dynamics of the Liquid State, Clarendon press, Oxford.
22. González D. J., L. E. González, J. M. López and M. J. Stott, 2002. Dynamical properties of liquid Al near melting: An orbital-free molecular dynamics study.*Phys. Rev. B,***65**, 184201:1-13.
23. Iida T. and R. I. L. Guthrie, 2015. The Thermophysical Properties of Metallic Liquids, Vol: **1** Fundamentals, Oxford University Press, Oxford.
24. Molla M. R., 2016. Study of the bulk properties of liquid transition metals. PhD Thesis, Department of Theoretical Physics, University of Dhaka.
25. Palmer B. J, 1994. Transverse-current autocorrelation function calculations of the shear viscosity of molecular liquids. *Phys. Rev. E,***49**, 359-366.
26. Balucani U., J. P. Brodholt, P. Jedlovszky and R. Vallauri, 2000. Viscosity of liquid water from computer simulations with a polarizable potential model. *Phys. Rev. E,***62**, 2971-2973.